ISSN 1062-8738, Bulletin of the Russian Academy of Sciences: Physics, 2017, Vol. 81, No. 7, pp. 822–826. © Allerton Press, Inc., 2017.
Original Russian Text © N.M. Kleinerman, V.V. Serikov, N.I. Vlasova, A.G. Popov, A. Kashyap, 2017, published in Izvestiya Rossiiskoi Akademii Nauk, Seriya Fizicheskaya, 2017, Vol. 81, No. 7, pp. 909–913.

Investigating Aspects of the Formation of Structure in FePd Alloy upon Ordering

N. M. Kleinerman[a], *, V. V. Serikov[a], N. I. Vlasova[a], A. G. Popov[a] , and A. Kashyap[b]

[a] *Mikheev Institute of Metal Physics, Ural Branch, Russian Academy of Sciences, Yekaterinburg, 620990 Russia*

[b] *Indian Institute of Technology Mandi, Kamand, Mandi (HP)-175005, India*

**e-mail:kleinerman@imp.uran.ru*

Abstract—The Mössbauer effect is used to study changes in the structure of $Fe_{50}Pd_{50}$ alloy in the course of annealing for ordering at $T = 450$°C from different initial states: cast and quenched from 950°C, then subjected to severe plastic deformation by shear under pressure, and that obtained by fast quenching from the melt. Differences in the kinetics of phase transformations are observed depending on the initial state of the material.

DOI: 10.3103/S1062873817070140

INTRODUCTION

Iron and cobalt alloys containing noble metals (CoPt, FePt, FePd) with the $L1_0$-type structure differ favorably from other highly anisotropic materials for permanent magnets due to their better corrosion resistance and good plasticity. Interest in these systems is nowadays associated with the search for materials for permanent magnets that do not contain noble elements. In contrast to CoPt and FePt, achieving potentially high hysteresis properties in a cheaper FePd alloy is fraught with great difficulties, and the level of coercive force H_c reached in bulk FePd samples even after severe plastic deformation and subsequent ordered annealing is very low [1] and far from the theoretical limit $H_a = 3.5$ T (where H_a is the field of magnetocrystalline anisotropy). Investigations with Mössbauer spectroscopy enable us to identify fine features of structural transformations, analysis of which could help us develop ways of improving magnetic characteristics. The aim of this work was to compare the structural changes that occur in the course of the annealing of $Fe_{50}Pd_{50}$ alloy at $T = 450$°C from different initial states: cast and quenched from 950°C, then subjected to severe plastic deformation; and that fast-quenched from melt alloy. The MSTOOLS software [2] was used to analyze the Mössbauer spectra.

EXPERIMENTAL

Coarse-grained polycrystalline rods 50 mm long and 6 mm in diameter, cast from FePd equiatomic alloy, were homogenized at a temperature of 950°C for 6 h and then quenched in ice water. Disk-shaped samples were cut from the disordered rods, parts of which were then subjected to severe plastic deformation by high pressure torsion (HPT) at number of revolutions $n = 5–10$ and high quasistatic pressure $P = 6$ GPa. Samples of fast-quenched alloy (FQA) FePd were prepared via casting melt on a wheel rotating at linear surface speed $V = 30$ m s^{-1} (MS-132). To perform our Mössbauer studies, the cast, fast-quenched, and strongly deformed FePd samples were thinned to a thickness of 25 μm and then annealed at a temperature of 450°C for 1–40 h. The Mössbauer spectra were measured at 300 K in the regime of constant accelerations with a Co^{57} source in a chromium matrix. Measurements were made on foils using an MC2201 spectrometer (512 channels; $(5–8) \times 10^5$ pulse/channel; coefficient of spectrum quality, 70–80). The spectra were treated using the MSTOOLS software [2] with allowance for the effects of self-absorption. Isomer shifts of the spectrum components were determined relative to an α-Fe spectrum.

RESULTS AND DISCUSSION

The dependences of the coercive force on the duration of annealing at $T = 450$°C are presented in Fig. 1 for the three different states of the alloy. The considerable differences between both the kinetics of growth and the maximum values of H_c that were achieved indicate that there are differences in the course of the transformation of the disordered face-centered $A1$-phase to the tetragonal ordered $L1_0$-phase between the deformed and quenched samples. In [3], the distribution of hyperfine fields (HFF) $P(H_{HFF})$ were used to analyze the Mössbauer spectra for the initial states after quenching and severe plastic deformation. It was shown that the structure of the cast alloys was strongly heterogeneous. Comparing it to the binomial distribu-

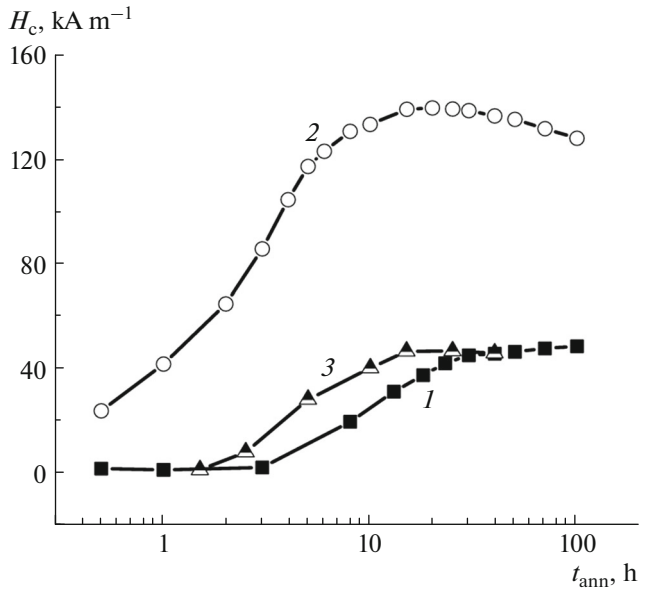

Fig. 1. Dependence of the coercive force on annealing time at $T = 450$°C for the samples of FePd alloy in different states: (*1*) cast alloy, (*2*) HPT, (*3*) FQA.

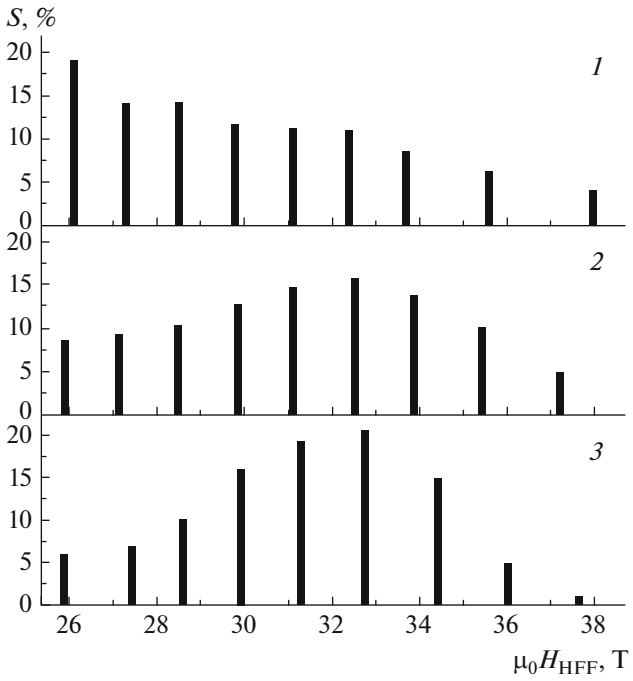

Fig. 2. Histograms of the distribution of relative fractions S of spectral contributions after the first annealing at $T = 450$°C for 1 h of samples of FePd alloy in different initial states: (*1*) cast alloy, (*2*) HPT, (*3*) FQA.

tion, we could see that it was no longer a uniform solid solution of one composition after additional plastic deformation, though it did have a smoother distribution $P(H_{HFF})$. The same can be said for the initial state after fast quenching.

However, despite the fact that the description of the changes in the alloy's structure using distributions $P(H_{HFF})$ restored from the Mössbauer spectra clearly demonstrates the differences in the kinetics of the separation of phase constituents from solid solutions, it provides no information on the local characteristics of these components (e.g., composition, volume fraction, or degree of lattice distortion). To determine these, we have to fit the spectra with individual (partial) spectral contributions that are characterized by certain values of hyperfine fields H_{HFF} and quadrupole shifts Q. The results from such treatment of the spectra for samples with different initial states are presented in Figs. 2–4 in the form of histograms of the distribution of relative areas S of the subspectra (the relative content of iron in different fields).

From Fig. 2, we can see that at the early stages of annealing, the histogram of distributions from each of the samples contain the lines of cubic components with the hyperfine field values close to $\mu_0 H_{HFF} = 34.4$, 33.0, 32.5, 31.0 T. As is known from [3], they correspond to low negative values of quadrupole shift ($|Q| < 0.1$ m s^{-1}). The specified HFF values belong to disordered regions with compositions close to Fe60Pd40, α-Fe, $Fe_{50}Pd_{50}$, and $Fe_{40}Pd_{60}$, respectively [3–6]. In addition, these histograms contain the lines from tetragonal components with different values of fields in the range of $\mu_0 H_{HFF} \approx 25.0$–30.0 T and positive Q. A comparison of the S values for tetragonal components after annealing for $t_{ann} = 1.0$ h (Fig. 2) shows that at the early stages of phase transformations, the formation of the $L1_0$ phase, which is characterized by the line with $\mu_0 H_{HFF} \approx 26.0$ T [3–6], is more intense in the cast sample ($S = 18\%$) than in the fast-quenched sample ($S = 6\%$). However, a gradual increase in the contribution with $\mu_0 H_{HFF} \approx 26.0$ T is observed upon subsequent annealings of the fast-quenched sample, and for the deformed sample as well [3]. At the same time, the structure of the cast sample is rearranged in a more complex manner.

Figures 3a, 3b respectively show the spectra and histograms of area S of the individual contributions at the different stages of annealing of cast samples. We can see that starting from duration of annealing $t_{ann} = 2.5$ h and up to 15 h, the redistribution of iron and palladium atoms takes place along with an increase in the relative fraction of areas with high values: $\mu_0 H_{HFF} > 30.0$; i.e., components with cubic lattices dominate in the sample structure. Only when $t_{ann} \geq 15$ h does the relative fraction of ordered regions close in the composition to the equiatomic sample begin to grow and dominate by volume, while the formation of heterogeneous tetragonal structures in fast-quenched and deformed samples annealed for 15 h is complete [3].

The histograms of the distribution of contributions to spectral intensity from different regions after $t_{ann} =$

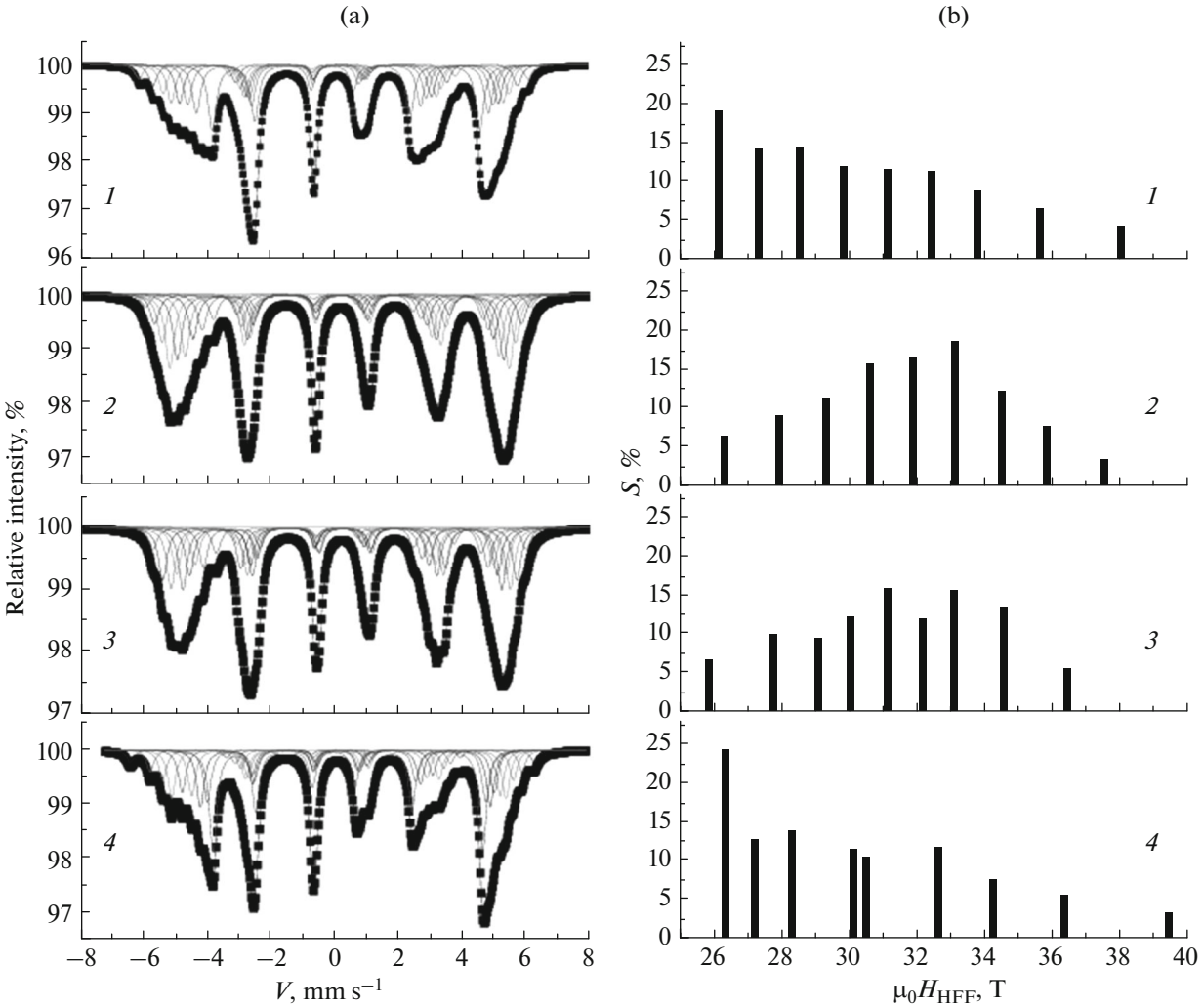

Fig. 3. (a) Spectra and (b) histograms of the cast sample after several annealings at $T = 450$°C: (*1*) 1, (*2*) 2.5, (*3*) 10, (*4*) 15 h.

40 h for the three initial samples (and for comparison, after $t_{ann} = 100$ h for the cast sample) are shown in Fig. 4a. The subsequent correlation dependences of the quadrupole shift Q and hyperfine field $\mu_0 H_{HFF}$ are presented in Fig. 4b. The relative fractions of disordered cubic components after the long-term annealing do not exceed in total 10 vol % for each sample. In the field range of $\mu_0 H_{HFF} \approx 25.0$–$30.0$ T, the histograms of distributions for each sample contain lines from tetragonal components with different values of $\mu_0 H_{HFF}$ and positive Q, testifying to the strong heterogeneity of the tetragonal structure of all samples.

If we limit ourselves to considering the fractions of contributions exceeding 5%, this barrier is overcome by six lines in the deformed sample. Since the first four lines from the tetragonal regions are positioned in the histogram with a fairly constant HFF shift (around 0.8 T per palladium atom in the second coordination shell and 1.5 T per iron atom in the first coordination shell), the main tetragonal components can presumably be identified.

In [3], the contribution with the maximum $Q \approx 0.44$–0.40 m s^{-1} and hyperfine field $\mu_0 H_{HFF} \approx 26.3$ T was attributed to the ordered $L1_0$ regions, which were characterized by a lack of iron atoms in the first coordination shell of the resonant atom and the atoms of palladium in the second shell. Another contribution with the maximum value Q and the lower value of $\mu_0 H_{HFF} \approx 25.5$ T yielded inclusions of palladium atoms in the second coordination shell, i.e., in the iron layer of ordered $L1_0$-phase. These regions with different environments of the resonant atom had virtually identical Q values throughout the annealing, indicating that they had the same tetragonal lattice.

The line with $\mu_0 H_{HFF} \approx 27.0$ T belongs to a configuration in which one iron atom is in a layer of palladium, and one palladium atom is in a layer of iron. This configuration should apparently be considered a

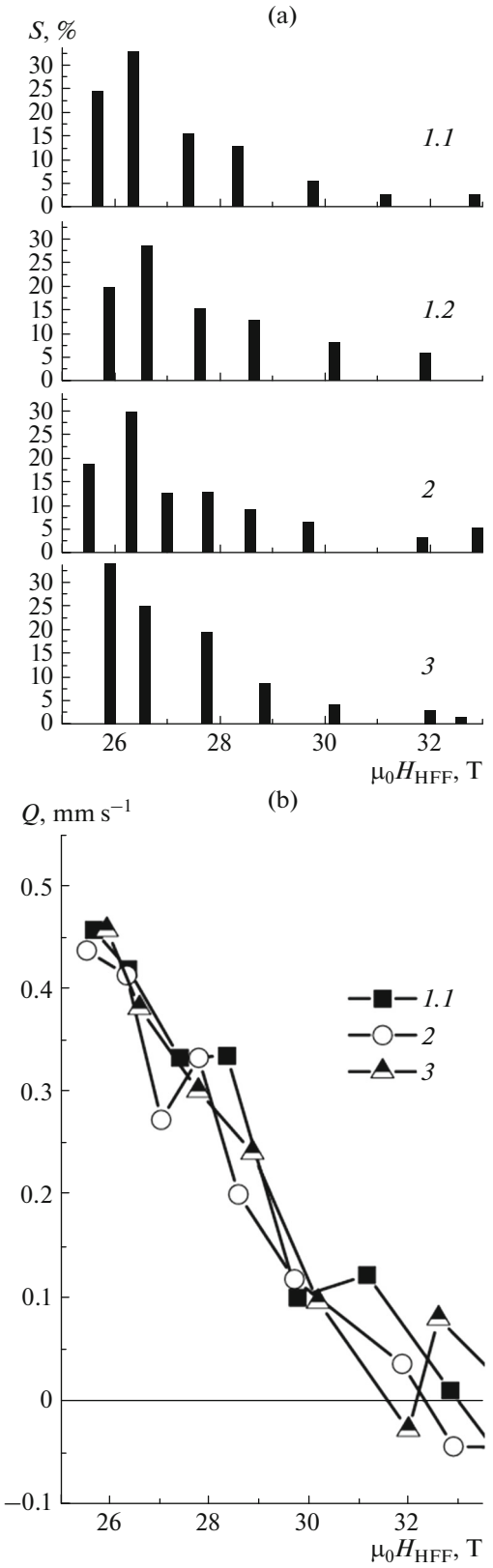

Fig. 4. Histograms of (a) the distributions of relative spectral contributions S and (b) the distribution curves of quadrupole shift Q by hyperfine fields for all samples in the final stages of annealing at $T = 450$°C: (*1.1*) cast alloy annealed for 40 h, (*1.2*) cast alloy annealed for 100 h, (*2*) HPT annealed for 40 h, (*3*) FQA annealed for 40 h.

tetragonal disordered phase. The tetragonal fcc disordered phase $A6$ was recently observed in the FePd and FeNi alloys [7, 8]. When a palladium atom is replaced by an iron atom in the first coordination shell, the hyperfine field grows by 1.6 T, compared to the HFF for the $L1_0$ phase. This results in the emergence of a line with a hyperfine field of $\mu_0 H_{HFF} \approx 28.0$ T in the Mössbauer spectrum, which apparently characterizes the environment of a resonant atom enriched in Fe. The large (but lower in value) quadrupole shifts of $Q \approx 0.30$ m s^{-1} correspond to such lines, showing that these coordinations can be attributed to isolated regions (phases) with the same tetragonal lattice.

As was shown in [9], the values of hyperfine fields in the range of $\mu_0 H_{HFF} \approx 29.0$–$30.0$ T correspond to a bcc phase with composition $Fe_{25}Pd_{75}$ in an $L1_2$-type ordered state. These hyperfine fields belong in our case to constituents with low values of the quadrupole shift: $Q \approx 0.15$ and 0.10 m s^{-1} (Fig. 4b). We may assume that the regions with compositions close to stoichiometric $FePd_3$ are tetragonally distorted, due to coherent bonds with other structural components. Based on the above, we may also assume that except for the classical ordered $L1_0$ phase, the deformed samples contain areas of the so-called modified $L1_0$ phase [10] enriched in one component or another (Pd or Fe), disordered tetragonal phase $A6$, and (in small amounts) the $L1_2$-type ordered phase.

The histograms of fast-quenched and cast samples differ from the described case in the number, intensity, and position of lines. This could be due either to differences in the numbers of different kinds of atoms in a specific configuration, or to differences in the spacing of atoms that belong to different structural constituents. In the cast sample subjected to the longest annealing ($t_{ann} = 100$ h), regions with the $L10$ structure formed similar to those formed in the deformed sample, which are presented by two lines in its histogram (Fig. 4). However, the total number of lines (5), their intensity, and the values of quadrupole shift differ from those of the deformed sample, testifying to the incomplete redistribution of elements between the structure components. Upon long-term annealing, changes can occur that negatively affect the magnetic characteristics of a structure (e.g., grain growth, stress relief, and the breaking of coherent bonds between structural components).

In the fast-quenched sample, there are four lines that may be considered intense. Regions that contribute to the only line with the maximum quadrupole shift $Q \approx 0.45$ m s^{-1} and belong to the ordered $L1_0$ phase form in 5 h. The relative fraction of these regions remains virtually the same upon further annealing. The nearly equidistant spacing of the HFFs of different lines for the fast-quenched sample can be explained by the smooth change in the concentration of the regions upon the emergence in their first and

second coordination shells of additional atoms of iron and palladium, and by the smooth reduction in the degree of tetragonality. The difference between quadrupole shifts also testifies to this (see Q (H_{HFF}) in Fig. 4b). Kinks in the dependences of the cast and deformed samples are clearly visible at $Q \approx 0.45$ and 0.30 m s^{-1}. There is no deviation from linearity for the fast-quenched sample. Even though the areas with the $L1_0$-type ordering display the most intense line, their role in the formation of anisotropic structure is diminished by the large volume of regions with reduced degrees of tetragonal distortions.

CONCLUSIONS

A comparative analysis of the results of our Mössbauer study revealed features of structural states that emerge upon annealing samples of the equiatomic FePd alloy from different initial states, allowing us to draw a number of conclusions.

1. The behavior of the Mössbauer parameters of the subspectra shows that upon the annealing of FePd alloy, tetragonal areas of intermediate compositions with different degrees of tetragonality form along with the $L1_0$ and $L1_2$ structural constituents. The observed patterns of cascade-type complex phase transitions [11] were common to all samples.

2. The volume fractions of different structural constituents in the fully formed structure depend on the initial state of sample.

3. The high volume fraction of regions with lower degrees of tetragonality (and thus reduced effective constant magnetocrystalline anisotropy) determined the value of coercive force H_c/H_a in all samples of FePd alloy.

ACKNOWLEDGMENTS

This work was supported by the Russian Academy of Sciences, Ural Branch, project no. 15-9-2-19; and by the Russian Foundation for Basic Research, project no. 17-52-45097.

REFERENCES

1. Vlasova, N.I., Gaviko, V.S., Popov, A.G., et al., *Solid State Phenom.*, 2011, vols. 168–169, p. 392.
2. Rusakov, V.S., *Messbauerovskaya spektroskopiya lokal'no neodnorodnykh sistem* (Mössbauer Spectroscopy of Locally Inhomogeneous Systems), Almaty: Inst. Yad. Fiz., 2000.
3. Vlasova, N.I., Kleinerman, N.M., Serikov, V.V., and Popov, A.G., *J. Alloys Compd.*, 2014, vol. 583, p. 191.
4. Longworth, G., *Phys. Rev.*, 1968, vol. 172, p. 572.
5. Tsurin, V.A., Ermakov, A.E., Lebedev, Yu.G., and Filippov, B.N., *Phys. Status Solidi*, 1976, vol. 33, p. 325.
6. Halley, D., Auric, P., Bayle-Guillemaud, P., et al., *J. Appl. Phys.*, 2002, vol. 91, p. 9757.
7. Vlasova, N.I., Popov, A.G., Shchegoleva, N.N., et al., *Acta Mater.*, 2013, vol. 61, p. 2560.
8. Montes-Arango, A.M., Marshall, L.G., Fortes, A.D., et al., *Acta Mater.*, 2016, vol. 116, p. 263.
9. Tsurin, V.A. and Men'shikov, A.Z., *Fiz. Met. Metalloved.*, 1978, vol. 45, no. 3, p. 547.
10. Litvinov, V.S. and Arkhangel'skaya, A.A., *Fiz. Met. Metalloved.*, 1977, vol. 43, no. 5, p. 1044.
11. Ni, Y., Jin, Y.M., and Khachaturyan, A.G., *Acta Mater.*, 2007, vol. 55, p. 4903.

Translated by A. Bannov